Available online at www.sciencedirect.com
SCIENCE DIRECT®
International Journal of Mass Spectrometry 227 (2003) 63–76
International Journal of Mass Spectrometry
www.elsevier.com/locate/ijms

Alkali metal binding energies of dibenzo-18-crown-6: experimental and computational results

Joseph D. Anderson, Eric S. Paulsen, David V. Dearden*

Department of Chemistry & Biochemistry, C100 Benson Science Building, Brigham Young University, P.O. Box 25700, Provo, UT 84602-5700, USA

Received 9 October 2002; accepted 28 October 2002

Abstract

We have experimentally bracketed the gas phase Li^+, Na^+, K^+, Rb^+, and Cs^+ affinities of dibenzo-18-crown-6 in the order 15-crown-5 (15C5) < dibenzo-18-crown-6 (DB18C6) < 18-crown-6 (18C6). Comparison with published experimental threshold collision-induced dissociation measurements yields enthalpies of binding at 298 K (in kJ mol^{-1}) as follows: DB18C6·Na^+, -299 ± 26; DB18C6·K^+, -221 ± 19; DB18C6·Rb^+, -154 ± 38; DB18C6·Cs^+, -136 ± 35 (experimental values for the bracketing ligands binding Li^+ are not available). Thus, dibenzo substitution of the crown makes it a weaker ligand toward the alkali metal ions, in contrast to dicyclohexano substitution, which was previously shown to make the crown a stronger ligand toward all the alkali metal ions. We have also calculated the enthalpies of binding between these metal ions and DB18C6 using both the LANL2DZ basis set and a modified version of the 6-31+G* basis set wherein diffuse functions are removed from carbon atoms and the K^+, Rb^+, and Cs^+ basis functions are those of the Hay–Wadt ($n + 1$) effective core potential set. Full geometry optimizations were carried out at the HF/6-31+G* and HF/LANL2DZ levels of theory, and energies were also calculated for the HF/6-31+G* geometries at the MP2(full)/6-31+G* and B3LYP/6-31+G* levels. The computed enthalpies of binding for the K^+, Rb^+, and Cs^+ complexes of DB18C6 fall between computed values in the literature for 15C5 and 18C6 complexes at both HF/6-31+G* and MP2(full)/6-31+G* levels, in good agreement with our bracketing experiments. The values at both levels of theory for the DB18C6 complexes of Li^+ and Na^+ are larger than those in the literature for both 15C5 and 18C6; the reasons for this discrepancy are not clear.

Keywords: Alkali metal; Crown ether; Gas phase

1. Introduction

Crown ethers are an important class of molecules of both inherent and practical interest. Since they were initially described by Pedersen in 1967 [1,2], they have been heavily studied in solution [3–5] and more recently they have also been examined in the gas phase. Among the earliest-recognized remarkable properties of these molecules is their ability to selectively bind metal cations in solution. This property is unusual but not unique; crown ethers mimic the ability of biological cation transport systems and of some antibiotics (such as valinomycin) that also bind metal cations selectively [6].

Crowns are of practical interest for a number of reasons. They have found application [7] in such diverse

* Corresponding author. Tel.: +1-801-378-2355; fax: +1-801-422-0153.
E-mail address: david_dearden@byu.edu (D.V. Dearden).

1387-3806/03/$ – see front matter © 2003 Elsevier Science B.V. All rights reserved.
doi:10.1016/S1387-3806(03)00042-3

Table 1
Comparison of complex stability constants for 18-crown-6 and dibenzo-18-crown-6 complexes with alkali metal ions in various solvents

Solvent	δ[b]	π^*[c]	$\log K$(18C6) $-\log K$(DB18C6)[a]		
			Na^+	K^+	Cs^+
Water	23.4	1.090	−0.6	0.4	0.1
Methanol	14.3	0.586	−0.1	1.1	1.1
Acetonitrile	11.7	0.713	−0.4	0.9	
Propylene carbonate	13.3		0.0	1.2	1.1
Dimethylsulfoxide	13.0	1.000	−0.4	0.7	1.7

[a] All data from [48].
[b] Hildebrand solvent polarity [49].
[c] Taft solvent polarity [49].

areas as selective transport and separation of metals, phase transfer catalysis and solvation of ions in nonpolar solvents, and stabilization of protonation sites in the electrospray ionization mass spectrometry of peptides [8,9]. Crown ethers are often cited as one of the key components in some of the most promising means of isolating radioactive components of nuclear waste [10–18].

Dibenzo-18-crown-6 (DB18C6 hereafter) was one of the first crown ethers described by Pedersen [1] and is a prototypical substituted crown. In solution, it has complexation properties similar to those of 18-crown-6 (18C6; see Table 1). Its aromatic substituents make it less soluble in aqueous media and increase its solubility in nonpolar solvents relative to 18C6. Therefore, it is often used when loss of ligand to an aqueous phase is a concern.

Probably because of its very low vapor pressure, DB18C6 has never been investigated in the gas phase, but it is desirable to do so for several reasons. One of the goals of our research is to characterize the intrinsic factors that affect cation recognition by crown ethers and other selective ligands. The most straightforward way to do this experimentally is to carry out studies in the gas phase, where complications arising from solvation are absent. For example, one of the questions we wish to address is whether or not DB18C6 is intrinsically a stronger ligand for alkali cations than 18C6. Formation constants measured in solution vary with solvent, method of measurement, and counterion present (for example, see Table 1), making it difficult to answer the question using solution data. In this paper, we wish to examine how substitution on the crown ring affects the intrinsic alkali cation affinities of the ligand. In an earlier study [19] that compared dicyclohexano-18-crown-6 (DC18C6) with 18C6 we found that the intrinsic affinities of the DC18C6 isomers for alkali cations are higher than those of 18C6 because of the higher polarizability of the substituted crown. DB18C6 is of interest because this ligand has a polarizability comparable to that of DC18C6 but is much more rigid than 18C6.

We also wish to examine the question of whether size match between the crown cavity and metal ion plays a role in enhancing the binding. The common explanation for the metal cation selectivities of crown ethers in solution is that crowns bind metals best that are the proper match to the size of the crown cavity [3,4]. However, such effects are not evident in the experimental metal ion binding energies measured in the gas phase [20–24]. We will use computational methods to address this question.

In this paper we present experimental results that bracket the gas phase affinities of DB18C6 for Li^+, Na^+, K^+, Rb^+, and Cs^+ between the affinities of 15-crown-5 (15C5) and 18C6 for the corresponding cations. We also deal with the question of how well computational chemistry can reproduce experimental results for these systems, where the energetic differences between the complexes being compared are small and the molecules are relatively large.

2. Experimental

2.1. Bracketing experiments

All experiments were performed using a Fourier transform ion cyclotron resonance mass spectrometer (model APEX 47e; Bruker Daltonics; Billerica, MA) that has been described previously [25,26]. The instrument is equipped with a microelectrospray ionization source modified [27] from an Analytica (Analytica of Branford; Branford, MA) design. The heated drying

tube is based on a design developed by the Eyler group at the University of Florida [28]. The instrument was controlled using a MIDAS [29] data system (National High Magnetic Field Ion Cyclotron Resonance Facility; Tallahassee, FL).

Bracketing experiments were performed for all the alkali metals simultaneously with a given crown. The ions were introduced into the instrument by electrospraying a "cocktail" solution containing the cations Li^+, Na^+, K^+, Rb^+, and Cs^+ and the ligand DB18C6. The concentrations of each salt and DB18C6 in the cocktail were 1×10^{-4} and 1×10^{-3} M, respectively, in acetonitrile. The salts were all alkali acetates except the cesium salt, which was the chloride. The lithium and rubidium salts were purchased from STREM Chemicals (Newburyport, MA), and sodium, potassium, and cesium salts were purchased from Mallinckrodt (Paris, KY). DB18C6 was purchased from Sigma Chemical Co. (St. Louis, MO). All were used as supplied without further purification. The ion source and transfer optics were tuned to maximize signal from the DB18C6·M^+ complexes. Neutral reactants were introduced into the ion trapping cell of the instrument using a controlled variable leak valve (12C4; from Aldrich; Milwaukee, WI) or a direct exposure vacuum lock probe (15C5 and 18C6; both from Parish Chemical; Orem, UT). The neutral reagent partial pressure as determined using a cold cathode ionization gauge was typically between 10^{-7} and 10^{-8} mbar during the bracketing experiments, but pressures were also further characterized using the proton transfer method described below.

The general procedure for the alkali cation affinity bracketing experiments involved electrospray of the "cocktail" solution described above to generate DB18C6·M^+ complexes of all the alkali cations. These were allowed to react for systematically varied time intervals with the neutral crown ether introduced via the vacuum lock, then the reaction products were probed. The reactant (R) and product (P) ion peak intensities for ions containing each of the alkali cations were extracted from the spectra; the ratio R/(R + P) was plotted as a function of reaction time. The slope of a plot of the natural log of R/(R + P) vs. time yields the reaction rates. For reactions involving 15C5, a more complicated procedure was followed because both cation transfer and ligand addition reactions were observed. In these cases, rate constants were obtained by fitting the data to a numerical solution of a coupled set of differential equations describing the system. Before and after each of these rate measurement experiments, the neutral crown ether was ionized via 70 eV electron impact, and similar rate measurements were carried out for the disappearance of the *m*/*z* 89 fragment ion (which corresponds to a molecular formula of $C_4H_9O_2^+$). This ion reacts via proton transfer to the neutral crown ether, and we assume the rate of this reaction to be collision-limited. Measurement of the proton transfer rates in this manner served to characterize the partial pressures of the neutral crowns in the ion trapping cell of the instrument.

2.2. Computational studies

The binding energy calculations consisted of Monte Carlo conformational searches with a molecular mechanics force field, followed by ab initio geometry optimization and energy computation as detailed below. Conformational searches were conducted using the Macromodel package, version 7.1 (Schrödinger, Inc., Portland, OR). We employed the AMBER* force field supplied with Macromodel and used the default MCMM method with automatic setup, except the force field was set for no electrostatic cutoffs and the number of Monte Carlo steps was set to 30,000.

The lowest-energy conformation found in the AMBER* conformational search was used as the starting point for ab initio geometry optimization. We recognize that the lowest energy conformers found in a molecular mechanics minimization will not necessarily be the lowest energy conformers according to higher levels of theory, but we expect any differences between the examined conformations and the global minima to be small. All of the higher-level calculations were set up and managed using the Ecce package (Pacific Northwest National Laboratory, Richland, WA) and used either the Gaussian 98 (versions A.6 and A.11; Gaussian Inc., Pittsburgh,

PA) (for Hartree–Fock geometry optimization and vibrational calculations) or NWChem (version 4.0; Pacific Northwest National Laboratory) (for MP2 and B3LYP energy calculations) computational engines. We employed two different basis sets for the calculations. The standard LANL2DZ basis set supplied with Ecce was used for calculations of all the alkali cation DB18C6·M^+ species. An additional set of calculations used the same basis set previously described by Feller and coworkers [30], which consists of the 6-31+G* basis functions on H, O, Li^+, and Na^+, the 6-31G* basis functions on C, and the Hay–Wadt MB $(n+1)$ effective core potential basis functions on K^+, Rb^+, and Cs^+. Following Feller's example, we will refer to this basis set as 6-31+G* for the remainder of this report, even though it is not strictly the 6-31+G* basis set of Pople. Binding energies were calculated as: $D(\mathrm{L}-\mathrm{M}^+) = E(\mathrm{LM}^+) - [E(\mathrm{L}) + E(\mathrm{M}^+)]$, where L is the ligand and M is the alkali metal. The MP2 and B3LYP calculations used the Ecce defaults except that the MP2 calculations did not use the frozen core approximation and that in the density functional calculations B3LYP was chosen as the combined exchange-correlation functional. Corrections to the HF and MP2 calculations were made for basis set superposition error using the counterpoise method [31], and thermal enthalpy corrections were made to all the calculations using vibrational frequencies calculated at the RHF/6-31+G* level of theory, assuming a temperature of 298 K.

3. Results

3.1. Exchange rates

Efficiencies of the metal exchange reactions from DB18C6 to other crown ethers (reaction 1), relative to the rates of exothermic proton transfer to the crowns, are listed in Table 2.

$$\mathrm{DB18C6}\cdot\mathrm{M}^+ + \mathrm{L} \rightarrow \mathrm{DB18C6} + \mathrm{L}\cdot\mathrm{M}^+ \qquad (1)$$

For L = 12C4, only the exchange reaction (reaction 1) was observed, but the efficiencies were all very low.

Table 2
Efficiencies for the reaction DB18C6·M^+ + L → DB18C6 + L·M^+

Metal	Ligand, L		
	12C4	15C5	18C6
Li^+	<0.002 ± 0.001	0.031 ± 0.003	0.33 ± 0.09
Na^+	<0.002 ± 0.001	0.011 ± 0.004	0.63 ± 0.09
K^+	0.041 ± 0.001	<0.002 ± 0.001	0.69 ± 0.07
Rb^+	0.057 ± 0.001	0.010 ± 0.010	0.70 ± 0.2
Cs^+	0.018 ± 0.001	0.020 ± 0.030	0.80 ± 0.2

No exchange was observed for M = Li or Na over the time scale of the experiment, which was up to 20 s. This leads to an estimated upper limit for the exchange reaction efficiencies for these metals of about 0.2%. The maximum observed exchange efficiency was for Rb^+, at 6%.

For L = 15C5, both exchange (reaction 1) and clustering (reaction 2) reactions were observed. The exchange efficiencies (Table 2) were all low, with a maximum of 3% for exchange of Li^+. Clustering was not observed for M = Li, but the efficiencies were 0.3 ± 0.1% for M = Na, 9 ± 3% for M = K, 15 ± 4% for M = Rb, and 13 ± 5% for M = Cs. We also observed $(15C5)_2\cdot M^+$ complexes for M = Na (4%), K (2%), Rb (16%), and Cs (7%) (efficiencies in parentheses). These complexes must be products of secondary reactions, either ligand addition to 15C5·M^+ or ligand exchange with (DB18C6)(15C5)·M^+. Thus, whereas exchange from DB18C6 to 15C5 was slow, clustering occurred at significant rates, especially for the larger metals.

$$\mathrm{DB18C6}\cdot\mathrm{M}^+ + \mathrm{L} \rightarrow (\mathrm{DB18C6})(\mathrm{L})\cdot\mathrm{M}^+ \qquad (2)$$

For L = 18C6, only the exchange reaction (reaction 1) was observed. The exchange efficiencies (Table 2) were significant for all the alkali cations, increasing monotonically from about 30% for M = Li to about 80% for M = Cs.

3.2. Computed structures of DB18C6·M^+ complexes

The conformational search procedure found a number of low-lying conformations for the free DB18C6

Table 3
AMBER*/Monte Carlo conformational search results

Species	No. of conformers found[a]	$\Delta(E_{min+1} - E_{min})$[b]
DB18C6	237	1.2
DB18C6·Li^+	64	0.6
DB18C6·Na^+	66	0.7
DB18C6·K^+	5	11.3
DB18C6·Rb^+	6	12.5
DB18C6·Cs^+	5	13.6

[a] Within 20 kJ mol^{-1} of minimum energy conformer.
[b] Difference in AMBER* strain energies between lowest and next lowest energy conformers (kJ mol^{-1}).

Table 4
Geometric parameters for DB18C6·M^+ complexes, computed at the RHF/LANL2DZ level

Metal, M	Angle between mean planes of benzene rings (°)	R (M − [mean O plane]) (Å)
Li	26.4	0.0447
Na	69.3	0.0774
K	54.8	0.7100
Rb	46.4	0.9977
Cs	38.9	1.5297

ligand and each of its complexes (Table 3). The number of low-lying conformers is greatest for the free ligand, decreases by a factor of about 4 for the Li^+ and Na^+ complexes, and is relatively small, with a large separation in energy between the lowest and next-lowest conformers, for the K^+, Rb^+, and Cs^+ complexes. Therefore, the likelihood that we have found the global minimum (and used it for subsequent higher-level calculations) is lowest for the free ligand and greatest for the K^+, Rb^+, and Cs^+ complexes.

The optimized structures of the DB18C6·M^+ complexes, determined at the RHF/LANL2DZ level, are shown in Fig. 1. Geometric parameters for the complexes, computed at the same level of theory, are listed in Table 4. The table gives the angle between the mean planes of the two benzene rings on the ligand, as well as the distance between the metal center and the mean plane of the ligand oxygen atoms. Use of the 6-31+G* basis set yielded qualitatively similar results.

The Li^+ and Na^+ complex structures are similar to each other and distinct from those of the K^+, Rb^+, and Cs^+ complexes. The DB18C6 ligand in the Li^+ and Na^+ complexes is highly twisted, in contrast to the structure found in an earlier molecular mechanics study [32] that also used the AMBER force field, which found boat-shaped structures with C_{2v} symmetry. That study used literature X-ray data to determine starting structures for the molecular mechanics minimizations and did not employ extensive conformational searching, which may account for its failure to find the twisted conformation depicted in Fig. 1. Beginning with a C_{2v} ligand and performing full geometry optimization at the RHF/6-31+G* level we arrive at a structure about 9 kJ mol^{-1} higher

Table 5
Computed total energies (Hartrees)[a] for DB18C6·M^+ complexes and related species

Species	Level of theory		
	HF/6-31+G*	HF/LANL2DZ	B3LYP/6-31+G*
Li^+	−7.23554	−7.23598	−7.28457
Na^+	−161.65929	0.00000	−162.08125
K^+	−27.70551	−27.70571	−27.97061
Rb^+	−23.44371	−23.44371	−23.70578
Cs^+	−19.47928	−19.47928	−19.73152
DB18C6	−1220.44762	−1220.10616	−1227.84091
DB18C6·Li^+	−1227.85241	−1227.53272	−1235.29109
DB18C6·Na^+	−1382.24087	−1220.25720	−1390.05394
DB18C6·K^+	−1248.25185	−1247.92619	−1255.90892
DB18C6·Rb^+	−1243.97489	−1243.64493	−1251.62991
DB18C6·Cs^+	−1239.99531	−1239.66198	−1247.64120

[a] No counterpoise or thermal corrections.

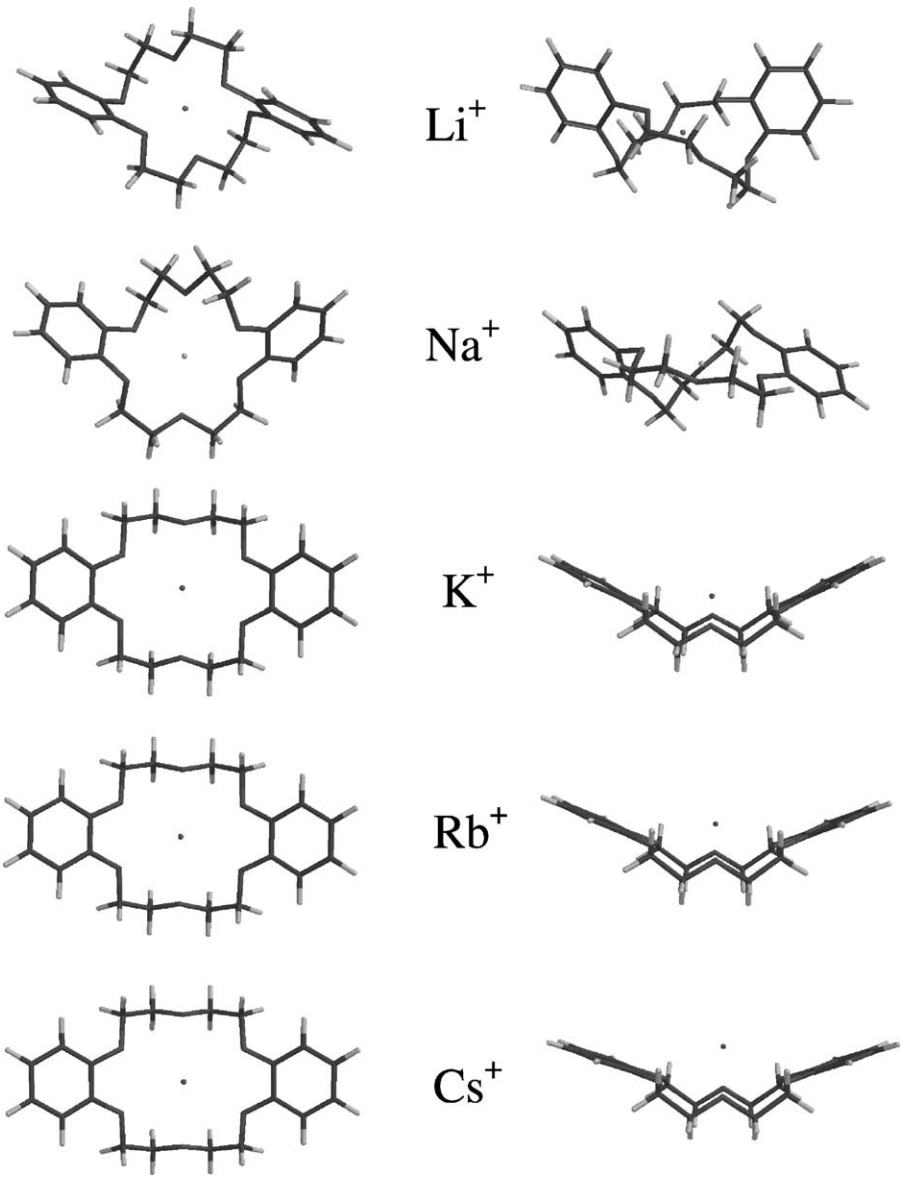

Fig. 1. Top (left) and side (right) views of DB18C6·M^+ complex structures computed at the RHF/LANL2DZ level.

in energy than the twisted conformer. The twisted conformer places the metal ion approximately at the centroid of the ligand oxygen atoms, allowing maximum interaction between the small, charge dense metal center and the electronegative donor groups of the ligand. It is possible that the twisted conformer is not the true global minimum, as the conformational search found many other conformations similar in energy.

The K^+, Rb^+, and Cs^+ complexes (Fig. 1) all have boat-shaped structures with C_{2v} symmetry, similar to the structures found in the earlier AMBER study [32]. In all of these structures the metal ion lies above the mean plane of the oxygen donor atoms. The height

Table 6
Computed and experimental enthalpies at 298 K for the reaction $L + M^+ \rightarrow LM^+$ (kJ mol^{-1})

Ligand, L	Method[a]	Li^+	Na^+	K^+	Rb^+	Cs^+
12C4	HF/6-31+G* [41]	−369	−265	−187	−154	−129
	MP2/6-31+G*	−359	−258	−196	−164	−140
	Threshold CID	−378 ± 51 [20]	−254 ± 13 [21]	−191 ± 11 [23]	−95 ± 13 [22]	−86 ± 9 [22]
15C5	HF/6-31+G* [42]	−430	−335	−234	−194	−162
	MP2/6-31+G*	−423	−320	−243	−204	−174
	Threshold CID [24]		−298 ± 18	−206 ± 14	−116 ± 6	−101 ± 6
18C6	HF/6-31+G* [30]	−364	−327	−283	−226	−183
	MP2/6-31+G*	−399	−336	−299	−243	−204
	Threshold CID [24]		−300 ± 19	−235 ± 13	−192 ± 13	−170 ± 9
DB18C6	HF/6-31+G*	−439	−336	−256	−213	−174
	HF/LANL2DZ	−479	−382	−291	−241	−194
	MP2/6-31+G*	−517	−388	−263	−229	−196
	B3LYP/6-31+G*	−429	−343	−253	−216	−178
	Bracketing of CID values[b]		−299 ± 26	−221 ± 19	−154 ± 38	−136 ± 35

[a] The designation "6-31+G*" indicates the Pople 6-31+G* basis set was used for all atoms except C, for which the diffuse functions were deleted, and K, Rb and Cs, for which the Hay–Wadt effective core potential basis set was used. "LANL2DZ" indicates the standard LANL2DZ basis set on all atoms.

[b] Average of threshold CID values for 15C5 and 18C6. Error bars are the greater of error propagation of threshold CID values or half the difference between values for 15C5 and 18C6.

of the metal center above the donor plane (Table 4) increases with increasing cation radius. In addition, the ligand "flattens" with increasing metal size, as can be noted from the decreasing trend in the angle between the benzene ring planes (Table 4) as the metal is varied. The large difference between these minimum energy conformers and the next-lowest conformers found in the search (Table 3) suggests a reasonable likelihood that these are the global minimum energy structures.

3.3. Computed energies of DB18C6·M^+ complexes

Total computed energies of the various DB18C6·M^+ complexes and related species at the Hartree–Fock and B3LYP levels of theory using the modified 6-31+G* basis set, and at the Hartree–Fock level using the LANL2DZ basis set, are listed in Table 5. These values were used to calculate enthalpies of metal binding to DB18C6, ΔH^{298}, and the results, along with enthalpies calculated at higher levels of theory, are reported in Table 6 with analogous values from the literature for 12C4, 15C5, and 18C6. The computed

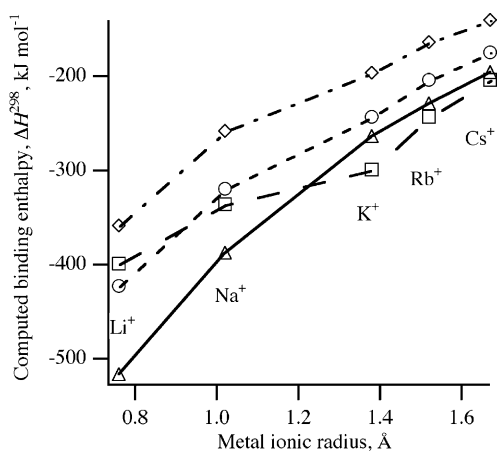

Fig. 2. Crown ether–alkali metal binding enthalpies (at 298 K, for the reaction crown + M^+ → crown·M^+) computed at the MP2(full)/6-31+G* level as a function of metal ionic radius. Diamonds (◇) represent crown = 12-crown-4 [41]. Circles (○) represent crown = 15-crown-5 [42]. Squares (□) represent crown = 18-crown-6 [30]. Triangles (△) represent crown = dibenzo-18-crown-6.

literature values were determined using the same basis sets we employed, and the experimental values were derived from threshold collision-induced dissociation measurements. The computed Hartree–Fock and MP2 values in Table 6 include counterpoise corrections [31] to account for basis set superposition error. The counterpoise corrections decreased the computed enthalpy of binding by 0–15 kJ mol^{-1} (with the largest correction for the Na^+ complex). The computed binding enthalpies (at the MP2(full)/6-31+G* level) for 15C5, 18C6, and DB18C6 are compared graphically in Fig. 2. For DB18C6, as found previously for the other crowns, the alkali cation binding energies decrease monotonically from Li^+ to Cs^+ using both basis sets. The LANL2DZ basis set yields binding enthalpies 20–50 kJ mol^{-1} greater than are obtained with the 6-31+G* basis set.

4. Discussion

4.1. DB18C6·M^+ binding energies

We have used the ion–molecule reaction bracketing method to experimentally determine the enthalpies of alkali metal binding by DB18C6 relative to other crown ethers. The assumption underlying this method is that exothermic reactions will occur rapidly, whereas endothermic reactions will not. For example, in proton transfer reactions in the absence of an activation barrier, reaction rates increase from less than 10^{-13} cm^3 molecule^{-1} s^{-1} up to the collision rate as ΔH° varies from about +20 to −20 kJ mol^{-1} [33].

Although we are dealing with the transfer of metal ions between ligands rather than simple proton transfer, the assumption of significant reaction efficiency for exothermic reactions and low efficiency for endothermic reactions is still reasonable for these metal transfer reactions. Metal transfers likely proceed through a long-lived collision complex. Often, crown ether–metal ion collision complexes are sufficiently long-lived that they are stabilized either through collisions with third bodies or through emission of radiation and are observed [34,35]. Because the collision complexes are long-lived, they are able to thoroughly explore phase space and overcome kinetic barriers that might otherwise distort the results. If the metal transfer is exothermic, energy will be released into the vibrational modes of the collision complex and this will promote relatively rapid dissociation of the complex, with the metal ion most likely remaining with the ligand for which it has higher affinity. If the transfer is endothermic, either the complex will be very long-lived such that it can be stabilized by collisions and/or emission of radiation, so that a cluster product will be observed, or it will be so weakly bound that it will dissociate back to reactants.

Table 2 indicates that the metal transfer reaction efficiencies from DB18C6 to 12C4 are all less than 6%, suggesting that these reactions are endothermic. This is not surprising given that 12C4 has two fewer donor atoms than DB18C6 and is far less polarizable (17.3 Å^3 for 12C4 and 37.7 Å^3 for DB18C6, estimated using the method of atomic hybrid components [36,37]). The situation is somewhat more complicated when comparing 15C5 with DB18C6, because both metal exchange (reaction 1) and clustering (reaction 2) are observed, with clustering efficiencies of about 10% or more for the complexes of K^+, Rb^+, and Cs^+. However, we believe alkali cation transfer from DB18C6 to 15C5 is still endothermic. The transfer efficiencies are all less than about 3%, and clustering indicates that whereas 15C5 has significant affinity for the metal ions the affinity is not large enough to release sufficient energy to promote rapid dissociation of the collision complexes, nor is it large enough to leave the metal attached to 15C5, displacing DB18C6; it is very likely less than the affinity of DB18C6 for the metal cations. It is interesting to note that clustering is only observed for the alkali cations that are about the same size or larger than the cavity of DB18C6, paralleling earlier observations with the unsubstituted crown ether–alkali cation complexes [34,35]. Clustering only occurs when the metal cation is large enough that it is not encapsulated by the DB18C6 ligand.

Alkali cation transfer from DB18C6 to 18C6 is relatively rapid, with observed efficiencies ranging from about 30 to about 80% as metal cation radius increases.

No clustering reactions involving these two ligands were observed. Thus, energy release in these reactions is large enough that collision complex dissociation occurs prior to stabilization. Based on the efficiencies of these reactions, all appear to be exothermic. Thus, the affinity of DB18C6 for each of the alkali metal ions is intermediate between those of 15C5 and 18C6.

Given that the affinities of DB18C6 for the alkali cations are between those of 15C5 and 18C6 for the corresponding metal ions, what are the absolute values for the DB18C6-alkali cation affinities? Two approaches might yield accurate values. Because absolute 15C5 and 18C6 affinities for Na^+, K^+, Rb^+, and Cs^+ have been measured using threshold CID methods [24], those values can be used in conjunction with the bracketing results to obtain estimates of the absolute DB18C6 alkali cation affinities. Alternatively, ab initio theory can be used to determine absolute values.

The measurement of kinetic energy thresholds for collision-induced dissociation (CID) is a well-established technique for bond energy determinations in isolated gas phase systems [38,39]. To determine accurate binding enthalpies, the raw reaction cross section measurements are corrected to allow for the thermal energies of the collision partners and for kinetic shifts in the threshold arising from the need for dissociation to occur rapidly enough to be observed on the time scale of the experiment [40]. These corrections have been found to generally produce excellent agreement with results from other methods, although the crown ether–alkali cation systems are larger, and in particular require larger kinetic shift corrections, than most other systems examined using threshold CID techniques.

The binding enthalpies of 12C4 for Li^+–Cs^+ [20–23], and of 15C5 and 18C6 for Na^+–Cs^+ [24] have been determined using the threshold CID technique and are listed in Table 6. Most are in reasonable agreement with the results of ab initio calculations (see Table 6 and discussion below), but some (in particular, those for 12C4 or 15C5 binding Rb^+ or Cs^+) show greater deviations from the ab initio values. In these cases, it is believed that the experiment may have probed an isomer less-strongly bound than the ground state isomer for which the calculation was performed. The reported binding enthalpies of 15C5 for each alkali cation are less than those of 18C6 for the same cations, although the difference for Na^+ is small. These values are consistent with the results of an earlier bracketing study [35], which found that for each alkali cation the ligand binding affinity is in the order 12C4 < 15C5 < 18C6.

Combining the results of the bracketing experiments with the threshold CID binding enthalpy determinations from the literature, the binding enthalpies of DB18C6 for Na^+–Cs^+ can be determined as the averages of the literature values for 15C5 and 18C6. These values are listed in Table 6, along with uncertainties determined from the greater of the propagated errors in the threshold CID values and half the difference between the reported values for 15C5 and 18C6. The binding enthalpies determined in this fashion for DB18C6 decrease monotonically from Na^+ to Cs^+ as expected based on the electrostatic nature of the interaction and the increasing size of the metal ions. The values for Rb^+ and Cs^+ determined this way are likely to be low, because of the suspected problems with the reported values for the binding of 15C5 to these metals [22].

Independently, the results of ab initio calculations can be used to determine absolute binding enthalpies. These values can be compared with the results of the bracketing experiments and with similar calculations in the literature. Published alkali cation binding enthalpies are available in the literature for 12C4 [41], 15C5 [42], and 18C6 [30], and these calculations employed some of the same methods (RHF and MP2) and basis sets (modified 6-31+G*) as we used, so the results should be directly comparable.

One question that should be addressed before making these comparisons deals with which level of theory should be used. In most cases, theoretical methods that include the effects of electron correlation, such as MP2 and B3LYP, give more accurate answers than RHF methods. However, for the crown ether/alkali cation complexes examined previously (see Table 6), the computed binding enthalpies are in general significantly larger than the values determined

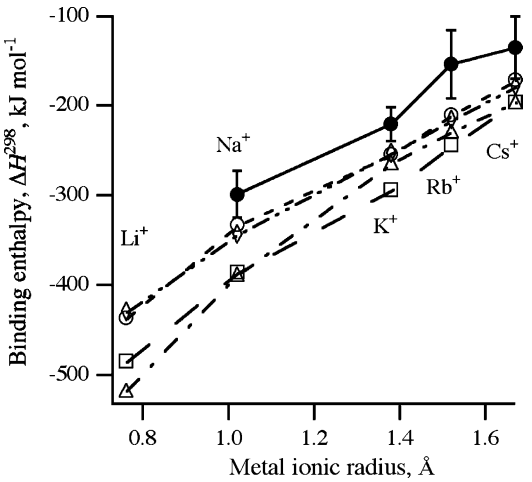

Fig. 3. Enthalpies (at 298 K) of alkali cation binding by dibenzo-18-crown-6. Solid circles (●) are averages of the threshold collision-induced dissociation values experimentally determined for 15-crown-5 and 18-crown-6. Open symbols represent computationally determined values: (○), RHF/6-31+G*; (□), RHF/LANL2DZ; (△), MP2/6-31+G*; (◇), B3LYP/6-31+G*.

using threshold collision-induced dissociation experiments, and the differences between experiment and theory are generally larger at the MP2 level than at the HF level. Binding enthalpies for DB18C6·M$^+$ systems determined by bracketing the threshold CID experimental values and computed at various levels of theory are compared graphically in Fig. 3. As with the other crowns, the experimental binding enthalpies are smaller than the computed ones. Of course, the experimental values here were derived from threshold CID measurements that also gave smaller values than were obtained computationally for the corresponding systems. The RHF/6-31+G* and B3LYP/6-31+G* computed values are very similar to each other for each of the metals and yield results closest to the experimental values. Surprisingly, the MP2/6-31+G* values are all larger and farther from the experimental values than the RHF/6-31+G* or B3LYP/6-31+G* values, especially for the Li$^+$ and Na$^+$ complexes. The RHF/LANL2DZ results roughly parallel the MP2/6-31+G* results. On the basis of comparison with the experimental results and the expected quality of the various levels of theory, we believe the B3LYP/6-31+G* computed values are probably the most accurate. The computed ΔH^{298} values for the Na$^+$ and K$^+$ complexes of DB18C6 agree with the CID-bracketed values about as well as the computed values for the 18C6 complexes agree with the CID values for 18C6. The agreement between the computed and CID-bracketed values is worse for the Rb$^+$ and Cs $^+$ complexes of DB18C6. It is likely that the bracketed values are low because of the acknowledged problems in the CID values for the 15C5 complexes.

The computed results for K$^+$, Rb$^+$, and Cs$^+$ at all levels of theory, presented in Table 6 and Fig. 2, are consistent with the bracketing results. In agreement with our experiments, the calculations find binding enthalpies for these metals in the order 15C5 < DB18C6 < 18C6. However, inconsistencies develop when the results for the smaller metal cations are considered.

The computed RHF/6-31+G* binding enthalpies for Na$^+$ by 15C5, 18C6, and DB18C6 are all similar, spanning a range of 8 kJ mol^{-1} (see Table 6). The published magnitude of ΔH^{298} for formation of 15C5·Na$^+$ [42] is greater than that for 18C6·Na$^+$ [30] by that amount. However, these theoretical results are inconsistent with a prior bracketing study that found Na$^+$ affinities in the order 15C5 < 18C6 [35], and with the current bracketing results, which find the order to be 15C5 < DB18C6 < 18C6. Further, they are weakly inconsistent with the threshold CID results (Table 6), which find affinities in the order 12C4 < 15C5 ≈ 18C6. Higher-level calculations [30,42] that include the effects of electron correlation (MP2/6-31+G*) are consistent with experiment. These calculations reverse the order of Na$^+$ affinities, placing that of 15C5 at −320 kJ mol^{-1} and that of 18C6 at −336 kJ mol^{-1}. However, the MP2/6-31+G* Na$^+$ affinity of DB18C6 is −388 kJ mol^{-1}, larger than that of 18C6, in disagreement with the current bracketing results. If the Na$^+$ affinities of 15C5 and 18C6 are as similar as suggested by the ab initio and threshold CID results, it should be possible to observe equilibrium in the Na$^+$ transfer reaction between these two ligands, although complications may arise because of the tendency of 15C5·Na$^+$ to add a second 15C5 ligand [35].

According to RHF/6-31+G* calculations, the binding enthalpies of Li^+ with 15C5 and DB18C6 are similar, but the reported value for 18C6·Li^+ is weaker by about 70 kJ mol^{-1} (see Table 6). At this level of theory, 18C6 binds Li^+ less well than does either 15C5 or 12C4. Again the theoretical results do not agree with the findings of either current or prior [35] bracketing experiments, which place the Li^+ binding enthalpies in the order 12C4 < 15C5 < DB18C6 < 18C6. The agreement between experiment and theory improves somewhat at the MP2/6-31+G* level; this level of theory puts ΔH^{298} at −359 kJ mol^{-1} for 12C4·Li^+, −423 kJ mol^{-1} for 15C5·Li^+, −399 kJ mol^{-1} for 18C6·Li^+, and −517 kJ mol^{-1} for DB18C6·Li^+, but the magnitude of the 18C6·Li^+ value is still too small to be consistent with the bracketing experiments.

The reason for the disagreements between experiment and theory for the smaller metal ions is unclear. It could be argued that the conformations selected from our searches were not the true global minima, but if lower energy conformations exist the computed binding enthalpies for them will be larger than those we have reported here and the disagreement with experiment will be larger. Comparing the trends in the computed binding enthalpies for the various crown ethers (Fig. 2), the 18C6·Li^+ and 18C6·Na^+ values appear inconsistently small. It is possible that the lowest energy conformers of these complexes were not found in the earlier calculations. In addition, it is well to remember that the experiments probe differences in free energies, whereas the computed values are for enthalpies. Binding a metal cation to a crown is entropically unfavorable because of the loss of degrees of freedom that occurs on complexation. If the entropic effects are more unfavorable for DB18C6 than for 18C6 (which seems unlikely, given the relative flexibilities of the two ligands), that might decrease the free energy of binding DB18C6 sufficiently to account for the results. Further, both the 18C6 and DB18C6 complexes of the smaller alkali cations have numerous low-lying conformations that likely are populated at thermal energies. If 18C6·M^+ has more populated low-lying conformers than DB18C6·M^+ (which seems likely, given the relative flexibilities of the two ligands) this would increase the relative cation affinity of 18C6 and might account for the differences between experiment and theory. In any event, further work is needed to resolve these disagreements.

4.2. Size effects in alkali cation binding by DB18C6

The correlation between solution binding constants and the "fit" of the metal cation in the crown cavity is well known [5,43]. In contrast, the gas phase enthalpies of binding generally decrease monotonically for a given crown as the cation size increases. Does size-matching play a role in the intrinsic binding of metal ions by crown ethers? The experimental values available so far have relatively large uncertainties, so subtle size effects, if present, are masked by experimental "noise." The computational data, on the other hand, offer hints that size matching may at least weakly influence cation binding. Examination of the computed enthalpies of binding as a function of cation radius for various crowns (Fig. 2) shows a smooth trend line for 12C4 and 15C5. For 18C6, on the other hand, there is a sharp break at K^+ (which may be accentuated by a high value for Li^+, as discussed above). With an ionic radius of 1.38 Å [44], K^+ is the best alkali cation match for the cavity of 18C6 (estimated cavity radius: 1.34–1.43 Å) [45]. Such a break is, however, not evident in the MP2/6-31+G* binding enthalpies computed for DB18C6. On the basis of their structural similarity, DB18C6 has a cavity radius similar to that of 18C6, but DB18C6 is less flexible and therefore less able to adapt to the size of a guest cation.

Consideration of the computed entropies of alkali cation binding by DB18C6 (Fig. 4) does suggest size matching effects. As expected based on the loss of translational and vibrational entropy that occurs when the complexes form, all the entropies of binding are unfavorable. The entropies show a break in the trend vs. metal ion radius at K^+; the value for K^+ is more unfavorable than would be expected on the basis of the trend for the other alkali cations. The idea of size matching rationalizes this result. Binding of K^+ is more unfavorable than the trend for the other metal

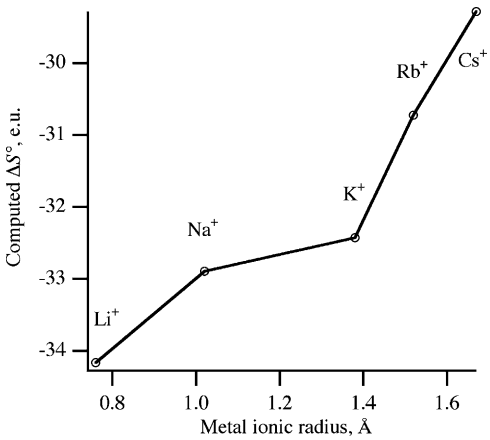

Fig. 4. Entropies (ΔS°, at 298 K) for the reaction DB18C6+M^+ → DB18C6·M^+ computed at the RHF/6-31+G* level of theory.

ions would suggest because K^+ fits tightest in the binding cavity of the crown and therefore binding K^+ results in the greatest loss of motional freedom.

The difference in energies between the lowest energy conformation of the free ligand and the conformation adopted on binding the metal ion also shows metal ion size effects. The ligand relaxation energies (Table 7) are large and comparable for the highly-twisted complexes of Li^+ and Na^+, and only about two-thirds as large for the more symmetric complexes of K^+, Rb^+, and Cs^+. An earlier computational study [46] of K^+ complexes of 18C6 and derivatives (including DB18C6) found a strong correlation between ligand relaxation energies for the complexes and complex stabilities. The same qualitative correlation is evident in our gas phase results.

Table 7
Entropies (ΔS°) and ligand relaxation energies computed at the RHF/6-31+G* level for the reaction DB18C6 + M^+ → DB18C6 · M^+

M	ΔS° (J mol^{-1} K^{-1})	Ligand relaxation energy (kJ mol^{-1})
Li	−34.2	125
Na	−32.9	122
K	−32.4	88
Rb	−30.7	87
Cs	−29.3	86

4.3. Influence of electronic effects and ligand rigidity on cation affinities

We can now compare three crown ligands with similar cavity sizes but differing degrees of rigidity and differing substituent electronic effects: 18C6, DC18C6, and DB18C6. Prior gas phase work [19] has shown that both isomers of DC18C6 have higher alkali cation affinities than 18C6, and that the isomers can be distinguished. DC18C6 is more rigid than 18C6, so the higher cation affinities of the former were attributed to the higher polarizability of DC18C6 (39.1 Å^3) relative to 18C6 (25.9 Å^3). We can now make the same kinds of comparisons for DB18C6.

DB18C6 has a higher polarizability (37.7 Å^3) than 18C6, but the aromatic rings make it much more rigid than either 18C6 or DC18C6. In most solvents (Table 1), the result is generally lower formation constants for binding K^+ or Cs^+ by DB18C6 than by 18C6. However, Na^+ binding constants are generally greater for DB18C6 than for 18C6.

Earlier work [47] with substituted DB18C6 ligands in solution suggests that electronic effects are important for metal binding by DB18C6 and provides precedent for changes in binding properties with guest cation size. This study found that solution alkali cation binding constants correlated with Hammett parameters such that greater substituent electron withdrawing power led to weaker complexes. Further, the electronic effects were greater for the K^+ complexes than for the Na^+ complexes. This was rationalized on the basis of the different sizes of these metal complexes. In the K^+ complexes, the metal interacts with all the oxygen donor atoms of the ligand, so if electron withdrawal occurs for any of the oxygen atoms the complex is weakened. In the Na^+ complexes, the smaller metal ion does not simultaneously interact with all the ligand oxygen atoms, so if binding to some of the oxygen atoms is weakened by electron withdrawing substituents the metal can simply shift coordination to a different oxygen atom that is not affected, maintaining stronger binding.

In the gas phase, all the electrostatic interactions are strengthened because there is no competition from

solvent. Therefore, it is likely that the lowest-energy gas phase conformations of DB18C6·Li^+ and DB18C6·Na^+ do involve coordination of all the ligand oxygen donor atoms (Fig. 1), so that electronic effects on the oxygen atoms adjacent to the aromatic rings do affect the complex stabilities. In addition, as noted above, DB18C6 is also more rigid (less conformationally mobile) than either 18C6 or DC18C6 and this might account for decreased cation affinity. The net result is that in the gas phase DB18C6 is a weaker ligand than 18C6 for all the alkali cations, not just the larger ones as observed in solution. The current experiments do not allow us to distinguish between electronic effects and the effects of decreased conformational mobility, but we note that from the RHF/6-31+G* calculations Mullikan charges on the O atoms in the DB18C6·Li^+ complex average 0.08 elementary charges greater than those in 18C6·Li^+, with the greatest charges on the phenolic O atoms and the smallest on the O atoms remote from the benzyl substituents. This suggests that ligand rigidity, rather than electronic effects, is probably the dominant factor.

5. Conclusions

The bracketing experiments indicate that despite its relatively high polarizability DB18C6 is a weaker ligand than 18C6 for each of the alkali metal ions. The higher rigidity of DB18C6, which prevents this ligand from optimally placing its donor atoms around the guest cation, is probably dominant in causing this, although electronic effects cannot be ruled out as an important factor. Electronic effects in this system could be further probed by examining the alkali cation affinities of DB18C6 substituted with electron donating or withdrawing groups on the benzene substituents.

Calculations using RHF, MP2, and B3LYP methods with a modified 6-31+G* basis set are consistent with both experiment and earlier calculations in predicting the order of ligand affinities for K^+, Rb^+, and Cs^+ to be 15C5 < DB18C6 < 18C6. However, the computed order of Li^+ affinities at all levels of theory is 18C6 < 15C5 < DB18C6, and that for Na^+ is 18C6 < DB18C6 < 15C5 (RHF) or 15C5 < 18C6 < DB18C6 (MP2), in contrast to the bracketing experiments, which give the same order as for the larger alkali cations. We do not currently have explanations for the disagreements; a more careful look should be taken at the Li^+ and Na^+ affinities of small crown ethers to try to rationalize the differences between experiment and theory. The computed entropies of complexation show weak evidence of the size match between the cavity of DB18C6 and K^+: trends in the entropies of complexation vs. cation size show a "dip" at K^+, suggesting a more unfavorable entropy of complexation than would be expected based on extrapolation from the values for the other alkali metal cations. However, these weak intrinsic effects do not account for the size selectivity observed in solution, which is a fortuitous combination of both intrinsic binding and differential solvation effects.

Acknowledgements

We are grateful to the donors of the Petroleum Research Fund, administered by the American Chemical Society, for support of this work. We are also grateful for the generous donations that have made the Ira and Marylou Fulton Supercomputing Center at Brigham Young University a reality, and wish to thank Professor Matt Asplund for his untiring help with our computational efforts.

References

[1] C.J. Pedersen, J. Am. Chem. Soc. 89 (1967) 2495.
[2] C.J. Pedersen, J. Am. Chem. Soc. 89 (1967) 7017.
[3] J.J. Christensen, D.J. Eatough, R.M. Izatt, Chem. Rev. 74 (1974) 351.
[4] R.M. Izatt, J.S. Bradshaw, S.A. Nielsen, J.D. Lamb, J.J. Christensen, D. Sen, Chem. Rev. 85 (1985) 271.
[5] R.M. Izatt, K. Pawlak, J.S. Bradshaw, R.L. Bruening, Chem. Rev. 91 (1991) 1721.
[6] M. Dobler, Ionophores and their Structures, Wiley, New York, 1981.
[7] G.W. Gokel, Crown Ethers and Cryptands, Royal Society of Chemistry, Cambridge, UK, 1991.
[8] S.W. Lee, H.N. Lee, H.S. Kim, J.L. Beauchamp, J. Am. Chem. Soc. 120 (1998) 5800.

[9] R.R. Julian, J.L. Beauchamp, Int. J. Mass Spectrom. 210/211 (2001) 613.
[10] P.V. Bonnesen, B.A. Moyer, D.J. Presley, V.S. Armstrong, T.J. Haverlock, R.M. Counce, R.A. Sachleben, Alkaline-Side Extraction of Technetium from Tank Waste Using Crown Ethers and Other Extractants, Oak Ridge National Laboratory, 1996.
[11] J.W. Grate, R. Strebin, J. Janata, O. Egorov, J. Ruzicka, Anal. Chem. 68 (1996) 333.
[12] J. Aupiais, C. Fayolle, P. Gilbert, N. Dacheux, Anal. Chem. 70 (1998) 2353.
[13] D.E. Katsoulis, Chem. Rev. 98 (1998) 359.
[14] G. Arena, A. Contino, A. Magri, D. Sciotto, G. Spoto, A. Torrisi, Ind. Eng. Chem. Res. 39 (2000) 3605.
[15] K. Kavallieratos, A. Danby, G.J. Van Berkel, M.A. Kelly, R.A. Sachleben, B.A. Moyer, K. Bowman-James, Anal. Chem. 72 (2000) 5258.
[16] C.M. Wai, B. Waller, Ind. Eng. Chem. Res. 39 (2000) 4837.
[17] T.G. Levitskaia, B.A. Moyer, P.V. Bonnesen, A.P. Marchand, K. Krishnudu, Z. Chen, Z. Huang, H.G. Kruger, A.S. McKim, J. Am. Chem. Soc. 123 (2001) 12099.
[18] S. Nishihama, T. Hirai, I. Komosawa, Ind. Eng. Chem. Res. 40 (2001) 3085.
[19] I.-H. Chu, D.V. Dearden, J. Am. Chem. Soc. 117 (1995) 8197.
[20] D. Ray, D. Feller, M.B. More, E.D. Glendening, P.B. Armentrout, J. Phys. Chem. 100 (1996) 16116.
[21] M.B. More, D. Ray, P.B. Armentrout, J. Phys. Chem. A 101 (1997) 831.
[22] M.B. More, D. Ray, P.B. Armentrout, J. Phys. Chem. A 101 (1997) 7007.
[23] M.B. More, D. Ray, P.B. Armentrout, J. Phys. Chem. A 101 (1997) 4254.
[24] M.B. More, D. Ray, P.B. Armentrout, J. Am. Chem. Soc. 121 (1999) 417.
[25] D.V. Dearden, C. Dejsupa, Y. Liang, J.S. Bradshaw, R.M. Izatt, J. Am. Chem. Soc. 119 (1997) 353.
[26] R.M. Pope, N. Shen, J. Nicoll, B. Tarnawiecki, C. Dejsupa, D.V. Dearden, Int. J. Mass Spectrom. Ion Process. 162 (1997) 107.
[27] N. Shen, R.M. Pope, D.V. Dearden, Int. J. Mass Spectrom. 195/196 (2000) 639.
[28] M. Wigger, J.P. Nawrocki, C.H. Watson, J.R. Eyler, S.A. Benner, Rapid Commun. Mass Spectrom. 11 (1997) 1749.
[29] M.W. Senko, J.D. Canterbury, S. Guan, A.G. Marshall, Rapid Commun. Mass Spectrom. 10 (1996) 1839.
[30] E.D. Glendening, D. Feller, M.A. Thompson, J. Am. Chem. Soc. 116 (1994) 10657.
[31] S.F. Boys, F. Bernardi, Mol. Phys. 19 (1970) 553.
[32] P.D.J. Grootenhuis, P.A. Kollman, J. Am. Chem. Soc. 111 (1989) 2152.
[33] G. Bouchoux, J.Y. Salpin, D. Leblanc, Int. J. Mass Spectrom. 153 (1996) 37.
[34] H. Zhang, I.-H. Chu, S. Leming, D.V. Dearden, J. Am. Chem. Soc. 113 (1991) 7415.
[35] I.H. Chu, H. Zhang, D.V. Dearden, J. Am. Chem. Soc. 115 (1993) 5736.
[36] K.J. Miller, J.A. Savchik, J. Am. Chem. Soc. 101 (1979) 7206.
[37] K.J. Miller, J. Am. Chem. Soc. 112 (1990) 8533.
[38] P.B. Armentrout, Thermochemical measurements by guided ion beam mass spectrometry, in: N.G. Adams, L.M. Babcock (Eds.), Advances in Gas Phase Ion Chemistry, vol. 1, JAI Press, Greenwich, CT, 1992, p. 83.
[39] P.B. Armentrout, Acc. Chem. Res. 28 (1995) 430.
[40] M.T. Rodgers, K.M. Ervin, P.B. Armentrout, J. Chem. Phys. 106 (1997) 4499.
[41] S.E. Hill, D. Feller, E.D. Glendening, J. Phys. Chem. A 102 (1998) 3813.
[42] S.E. Hill, D. Feller, Int. J. Mass Spectrom. 201 (2000) 41.
[43] J.D. Lamb, R.M. Izatt, S.W. Swain, J.J. Christensen, J. Am. Chem. Soc. 102 (1980) 475.
[44] R.D. Shannon, Acta Crystallogr. Sect. A: Found. Crystallogr. 32 (1976) 751.
[45] N.K. Dalley, R.M. Izatt, J.J. Christensen (Eds.), Synthetic Multidentate Macrocyclic Compounds, Academic, New York, 1978, p. 207.
[46] B.P. Hay, J.R. Rustad, C.J. Hostetler, J. Am. Chem. Soc. 115 (1993) 11158.
[47] K.H. Pannell, W. Yee, G.S. Lewandos, D.C. Hambrick, J. Am. Chem. Soc. 99 (1977) 1457.
[48] I.M. Kolthoff, M.K. Chantooni Jr., Anal. Chem. 52 (1980) 1039.
[49] T.H. Lowry, K.S. Richardson, Mechanism and Theory in Organic Chemistry, 2nd ed., Harper & Row, New York, 1981.